P H Y S I C A L   R E V I E W   L E T T E R S

Directed Percolation Criticality in Turbulent Liquid Crystals

Kazumasa A. Takeuchi,[1,*] Masafumi Kuroda,[1] Hugues Chaté,[2] and Masaki Sano[1,†]

[1]*Department of Physics, The University of Tokyo, 7-3-1 Hongo, Bunkyo-ku, Tokyo, 113-0033, Japan*
[2]*Service de Physique de l'État Condensé, CEA-Saclay, 91191 Gif-sur-Yvette, France*

We experimentally investigate the critical behavior of a phase transition between two topologically different turbulent states of electrohydrodynamic convection in nematic liquid crystals. The statistical properties of the observed spatiotemporal intermittency regimes are carefully determined, yielding a complete set of static critical exponents in full agreement with those defining the directed percolation class in $2 + 1$ dimensions. This constitutes the first clear and comprehensive experimental evidence of an absorbing phase transition in this prominent nonequilibrium universality class.

Transitions into an absorbing state, i.e., a state from which a system can never escape, arise from simple mechanisms expected to be widespread in nature. Examples abound in a wide variety of situations in physics and beyond [1], ranging from spreading processes like epidemics and forest fires, to spatiotemporal chaos, catalytic reactions, and calcium dynamics in cells, etc. Moreover, a host of problems, such as synchronization [2], self-organized criticality [3], and wetting [4], can be mapped onto them. Having no equilibrium counterparts, absorbing phase transitions are central in the ongoing search for the relevant ingredients determining universality out of equilibrium.

Over the past 25 years or so, it has been well established both in theory and in simulations that the vast majority of absorbing phase transitions share the same critical behavior, constituting the so-called directed percolation (DP) universality class [1]. This is not surprising since the DP class corresponds to the simplest case of a single effective absorbing state in the absence of any extra symmetry or conservation law, as conjectured by Janssen and Grassberger [5,6] and demonstrated by hundreds of numerical models [1].

However, the situation is quite different at the experimental level. Searching for evidence of DP critical behavior, a string of experiments have been performed [7], but the results remained unsatisfactory: they could not yield a complete set of critical exponent values in agreement with those defining the DP class (Table S1 [8]). In view of this state of affairs, the importance of finding at least one fully convincing experimental realization of DP-class scaling has been stressed [9]. The main difficulty probably stems from the fact that one must exclude long-range interactions [1], work with macroscopic systems to tame quenched disorder [10], and study them over long enough scales so that the critical behavior is unambiguously measured. We have overcome these difficulties and report here on a clear experimental observation of DP criticality.

We chose to work within electrohydrodynamic (EHD) convection regimes, which occur when a thin layer of nematic liquid crystals is subjected to an external voltage strong enough to trigger the Carr-Helfrich instability [11]. One advantage of this system is that very large aspect ratios can easily be realized, and that typical time scales are small (of the order of 10 ms). We focused on a transition between two topologically different turbulent states, called dynamic scattering modes 1 and 2 (DSM1 and DSM2), observed successively as V, the amplitude of the voltage, is increased [11,12]. The difference between the two states lies in their density of topological defects in the director field [Fig. 1(a)]. In the DSM2 state, these defects, called disclinations, are created and elongated considerably due to shear, leading to the loss of macroscopic nematic order and to a lower light transmittance. In DSM1, they are hardly elongated and their density remains very low.

Our quasi-two-dimensional cell is made of two parallel glass plates separated by a polyester film spacer of thickness $d = 12$ μm. The inner surfaces are covered with transparent electrodes of size 14 mm × 14 mm, coated with polyvinyl alcohol and then rubbed in order to orient the liquid crystals planarly in the x direction. The cell is filled with *N*-(4-methoxybenzylidene)-4-butylaniline (MBBA) doped with 0.01 wt. % of tetra-*n*-butylammonium bromide, maintained at temperature 25 °C with a standard deviation of 2×10^{-4}°C, and illuminated by a stabilized light source made of white light-emitting diodes. A CCD camera records the light transmitted through the plates. The observed region is a central rectangle of size 1217 μm × 911 μm. Since there is a minimum linear size of DSM2 domains, namely, $d/\sqrt{2}$ [12], we can roughly estimate the number of degrees of freedom to be 1650 × 1650 for the convection area and 143 × 107 for the observation area. Note that the meaningful figure is that of the total system size, which is at least 4 orders of magnitude larger than in earlier experimental studies [7]. In the following, we vary V and fix the frequency at 250 Hz, roughly one-third of the cutoff frequency 820 ± 70 Hz.

Closely above the threshold V_c marking the appearance of DSM2, a regime of spatiotemporal intermittency (STI) is observed, with DSM2 patches moving around in a DSM1
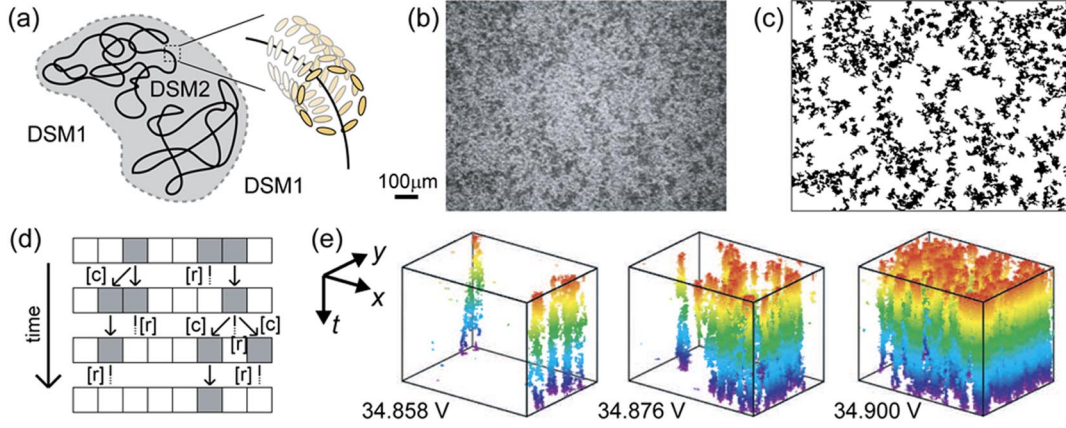
FIG. 1 (color online).   Spatiotemporal intermittency between DSM1 and DSM2. (a) Sketch of a DSM2 with its many entangled disclinations, i.e., loops of singularities in orientations of liquid crystals. (b) Snapshot taken at 35.153 V. Active (DSM2) regions appear darker than the absorbing DSM1 background. See also Movie S1 [8]. (c) Binarized image of (b). See also Movie S2 [8]. (d) Sketch of the dynamics: DSM2 domains (gray) stochastically contaminate [c] neighboring DSM1 regions (white) and/or relax [r] into the DSM1 state, but do not nucleate spontaneously within DSM1 regions (DSM1 is absorbing). (e) Spatiotemporal binarized diagrams showing DSM2 regions for three voltages near the critical point, namely, 34.858, 34.876, and 34.900 V. The diagrams are shown in the range of 1206 μm $\times$ 899 μm (the whole observation area) in space and 6.6 s in time.

background [Fig. 1(b) and Movie S1 [8]]. This suggests an absorbing phase transition [13] with DSM1 playing the role of the absorbing state [Fig. 1(d)]. Prior to any analysis, we must distinguish DSM2 domains from DSM1. This binary reduction can be easily performed by our eyes, so we automated it using the facts that DSM2 regions look darker, have longer time correlation, and have minimum area of $d^2/2$ [12] (see Ref. [8] for details). A typical result is shown in Fig. 1(c) and Movie S2 [8]. Figure 1(e) shows spatiotemporal diagrams obtained by that means in the steady STI state. They illustrate that the key ingredient is present: active DSM2 patches evolve in space-time essentially by contamination of the DSM1 absorbing state and recession from the DSM2 state [as sketched in Fig. 1(d)]. In this context, the order parameter ρ is just the ratio of the surface occupied by active (DSM2) regions to the whole area.

We first observe the steady-state STI regime under constant voltages V, in the range of 34.858 V $\leq V \leq$ 39.998 V. The voltage for the onset of steady roll convection is $V^* = 8.95$ V. The time average of ρ in the steady state, $\bar{\rho}$, is taken over the period 1000 s $< T <$ 8000 s, which is longer than 1000 correlation times. It shows a continuous and algebraic decay to zero with decreasing V, a clear signature of criticality (Fig. 2). The critical voltage V_c and the critical exponent β are determined by fitting these data to the usual form $\bar{\rho} \sim (V^2 - V_c^2)^\beta$. (Here, deviations from criticality are measured in terms of V^2 instead of V by convention, since the dielectric torque that drives the convection is proportional to V^2 [11].) This yields the following estimates:

$$V_c = 34.856(4) \text{ V}, \qquad \beta = 0.59(4), \qquad (1)$$

where the numbers in parentheses indicate the uncertainty

in the last digits, which correspond here to a 95% confidence interval in the sense of Student's t. Our estimate $\beta = 0.59(4)$ is in good agreement with the (2 + 1)-dimensional DP value $\beta^{DP} = 0.583(3)$ [14].

We then measure $N(l)$ and $N(\tau)$, the distributions of the sizes l and durations τ of the inactive (DSM1) regions. For instance, the distribution $N(l_x)$ in the x direction is obtained by detecting all inactive segments in the x direction for all y and t. We find that they decay algebraically at criticality up to a finite-size exponential cutoff [Figs. 3(a)– 3(c)]. The power-law decay is fitted as $N(l) \sim l^{-\mu_\perp}$ and $N(\tau) \sim \tau^{-\mu_\parallel}$ with
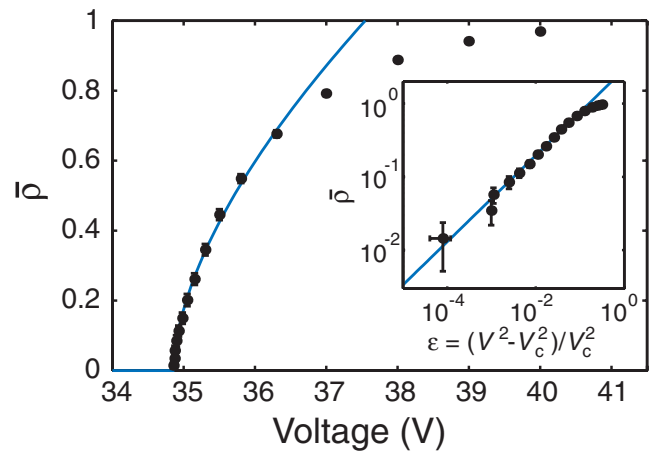

FIG. 2 (color online).   Variation of the average DSM2 fraction $\bar{\rho}$ with V in the steady state. Inset: same data in logarithmic scales, with vertical error bars indicating the standard deviation of the time series $\rho(t)$. Fluctuations of V are negligible except for the first data point, where the standard deviation is shown by a horizontal error bar. Solid lines are fitting curves.
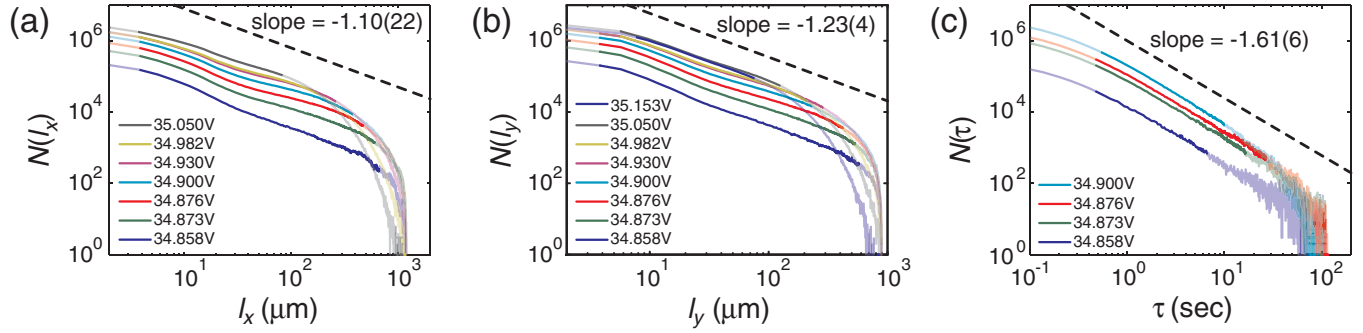
FIG. 3 (color online).   Histograms of inactive (DSM1) lengths l_x, l_y and duration τ in the steady state near criticality. Regions discarded in the fitting are painted light in color. Dashed lines indicate the estimated algebraic decay at threshold.

$$\mu_x = 1.10(22), \qquad \mu_y = 1.23(4), \qquad \mu_\parallel = 1.61(6), \tag{2}$$

where μ_x and μ_y indicate the exponent $\mu_\perp$ measured in the x and y direction, respectively. They are again in good agreement with the DP values $\mu_\perp^{DP} = 1.204(2)$ and $\mu_\parallel^{DP} = 1.5495(10)$ [14]. These exponents are related to the more conventional correlation length and time exponents $\nu_\perp$ and $\nu_\parallel$ via $\mu_\perp = 2 - \beta/\nu_\perp$ and $\mu_\parallel = 2 - \beta/\nu_\parallel$, which lead us to estimate

$$\nu_x = 0.66(17), \qquad \nu_y = 0.77(7), \qquad \nu_\parallel = 1.51(25). \tag{3}$$

They should be compared to the DP values $\nu_\perp^{DP} = 0.733(3)$ and $\nu_\parallel^{DP} = 1.295(6)$ [14]. The above estimates for $\nu_\perp$ are in reasonably good agreement with the DP value, while the agreement on $\nu_\parallel$ is less satisfactory. Our second set of experiments provides another, independent estimate of $\nu_\parallel$.

Setting the voltage to 60 V, i.e., much higher than V_c, we wait until the system is totally invaded by DSM2 domains. We then suddenly decrease V to a value in the range of 34.86 V $\leq V \leq$ 35.16 V, i.e., near V_c, and observe the time decay of activity for 900 s. We repeat this 10 times for each V value and average the results over this ensemble. In such "critical-quench experiments," correlation lengths and times grow in time, and, as long as they remain much smaller than the system size, the scaling estimates are free from finite-size effects. As expected, $\rho(t)$ decays exponentially with a certain correlation time for $V \leq$ 35.02 V, algebraically over the whole observation time for $V = 35.04$ V, and converges to a finite value for $V \geq$ 35.06 V [Fig. 4(a)]. A simple scaling ansatz implies the following functional form for $\rho(t)$ in this case:

$$\rho(t) \sim t^{-\alpha} f(\varepsilon t^{1/\nu_\parallel}), \qquad \alpha = \beta/\nu_\parallel, \tag{4}$$

where $\varepsilon = (V^2 - V_c^2)/V_c^2$ is the deviation from criticality and $f(\zeta)$ is a universal scaling function. From the slopes of the algebraic regimes for the three V values closest to the threshold, we estimate

$$V_c = 35.04(2)\text{V}, \qquad \alpha = 0.50_{-(5)}^{+(8)}. \tag{5}$$

Note that V_c is slightly higher than in the steady-state experiments. In fact, the roll convection onset $V^* = 8.96$ V is
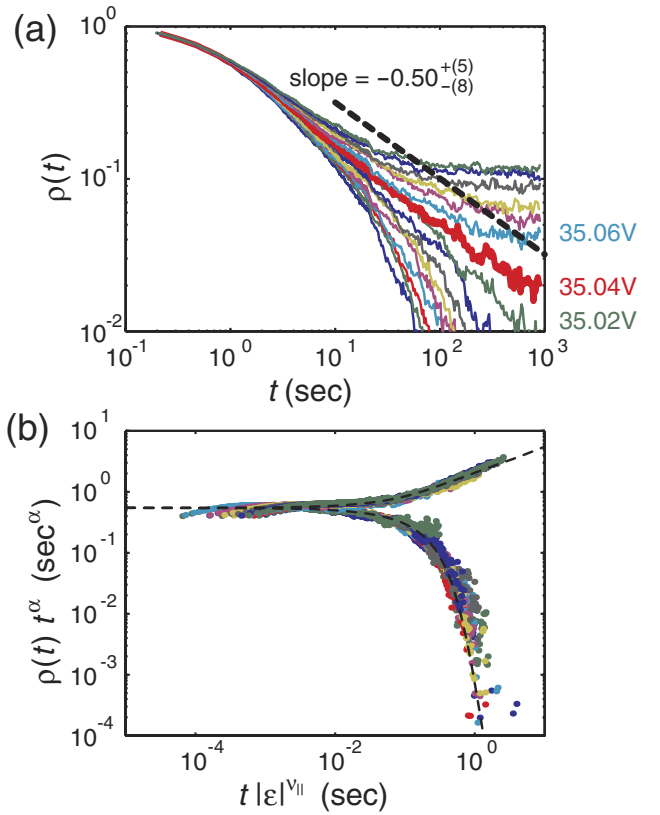

FIG. 4 (color online).   Critical-quench experiments. (a) Decay of $\rho(t)$ after the quench, for $V = 34.86$ V, 34.88 V, ..., 35.16 V from the bottom left to the top right. The data for $V = 35.04$ V (showing the longest scaling) are indicated by a thicker line. (b) Scaling plot of data in (a), with V_c, α, and $\nu_\parallel$ values estimated from the experiment [Eqs. (5) and (6)]. The dashed curve indicates the DP universal scaling function $f(\zeta)$ obtained numerically from the process sketched in Fig. 1(d) (so-called contact process). A collapse of similar quality is obtained when using DP-class exponent values.

also higher. We believe this is because, during the few days which separated the two sets of experiments, our sample has aged, a well-known property of MBBA. On the other hand, no measurable shift was detected during a given set of experiments. Our α value is again in good agreement with the DP value $\alpha^{\mathrm{DP}} = 0.4505(10)$ [14]. Finally, our direct estimates of β and α in Eqs. (1) and (5) and the scaling relation (4) yield

$$\nu_\| = 1.18^{+(14)}_{-(21)}, \qquad (6)$$

which is in good agreement with the DP value $\nu_\|^{\mathrm{DP}} = 1.295(6)$ [14]. Note that our two estimates of $\nu_\|$ lie on opposite sides of the DP value, with their confidence intervals overlapping this reference number. Furthermore, Eq. (4) implies that the time series $\rho(t)$ for different voltages collapse on the universal function $f(\zeta)$ when $\rho(t)t^\alpha$ is plotted as a function of $t|\varepsilon|^{\nu_\|}$. Our data do collapse reasonably well on the universal function of DP [Fig. 4(b)].

Continuous absorbing phase transitions are characterized by three independent (static) exponents [1]. So far, we have found those three independent algebraic scaling laws (typically over two decades). The critical exponent values all agree within a few percent with those of the DP class in $2 + 1$ dimensions. In addition, data collapse is satisfactorily achieved onto the universal scaling. This constitutes the first complete and unambiguous experimental realization of a DP-class absorbing phase transition [15]. Looking back at previous attempts to exhibit a DP phase transition experimentally, one may wonder why we obtained such clear DP scaling laws compared with earlier experiments (see Table S1 [8]). A major reason, already mentioned, is that EHD convection offers effective sizes orders of magnitude larger than in previously studied systems such as Rayleigh-Bénard convection. Similarly, typical time scales are much shorter. But beyond those obvious facts, we believe that our unusual choice of a transition between two fluctuating states has also helped: in many past experiments, the absorbing state was essentially fluctuation-free (laminar) [7] and thus may have caused long-range effects (mean flows and rigidity of the laminar pattern), which probably further reduced the effective size of the systems and could even break DP universality [1]. In our system, such long-range interactions are likely to be killed by local turbulent fluctuations of the absorbing state. In short, our experimental setup easily reveals DP scaling because it is able to tame both quenched disorder (being macroscopic) and long-range interactions (being turbulent).

The authors are grateful to S. Kai and S. Sasa for useful discussions. We also thank N. Oikawa, Y. Murayama, and S. Tatsumi for their advice on experiments. This work is partially supported by Japanese Grant-in-Aid for

———

*kazumasa@daisy.phys.s.u-tokyo.ac.jp
†sano@phys.s.u-tokyo.ac.jp

[1] H. Hinrichsen, Adv. Phys. **49**, 815 (2000).
[2] V. Ahlers and A. Pikovsky, Phys. Rev. Lett. **88**, 254101 (2002).
[3] R. Dickman, M. A. Muñoz, A. Vespignani, and S. Zapperi, Braz. J. Phys. **30**, 27 (2000).
[4] F. Ginelli *et al.*, Phys. Rev. E **68**, 065102(R) (2003).
[5] H. K. Janssen, Z. Phys. B **42**, 151 (1981).
[6] P. Grassberger, Z. Phys. B **47**, 365 (1982).
[7] S. Ciliberto and P. Bigazzi, Phys. Rev. Lett. **60**, 286 (1988); F. Daviaud, M. Bonetti, and M. Dubois, Phys. Rev. A **42**, 3388 (1990); S. V. Buldyrev *et al.*, Phys. Rev. A **45**, R8313 (1992); S. Michalland, M. Rabaud, and Y. Couder, Europhys. Lett. **22**, 17 (1993); H. Willaime, O. Cardoso, and P. Tabeling, Phys. Rev. E **48**, 288 (1993); M. M. Degen, I. Mutabazi, and C. D. Andereck, Phys. Rev. E **53**, 3495 (1996); P. W. Colovas and C. D. Andereck, Phys. Rev. E **55**, 2736 (1997); H. Téphany, J. Nahmias, and J. A. M. S. Duarte, Physica (Amsterdam) **242A**, 57 (1997); A. Daerr and S. Douady, Nature (London) **399**, 241 (1999); P. Rupp, R. Richter, and I. Rehberg, Phys. Rev. E **67**, 036209 (2003); C. Pirat, A. Naso, J.-L. Meunier, P. Maïssa, and C. Mathis, Phys. Rev. Lett. **94**, 134502 (2005).
[8] See EPAPS Document No. E-PRLTAO-99-056749 for the binarization algorithm, Movies S1 and S2, and Table S1. For more information on EPAPS, see http://www.aip.org/pubservs/epaps.html.
[9] P. Grassberger, in *Nonlinearities in Complex Systems*, edited by S. Puri and S. Dattagupta (Narosa, New Delhi, 1997), p. 61; H. Hinrichsen, Braz. J. Phys. **30**, 69 (2000).
[10] J. Hooyberghs, F. Iglói, and C. Vanderzande, Phys. Rev. Lett. **90**, 100601 (2003).
[11] P. G. de Gennes and J. Prost, *The Physics of Liquid Crystals* (Oxford University Press, Oxford, 1993), 2nd ed.
[12] S. Kai, W. Zimmermann, M. Andoh, and N. Chizumi, J. Phys. Soc. Jpn. **58**, 3449 (1989); Phys. Rev. Lett. **64**, 1111 (1990).
[13] Y. Pomeau, Physica (Amsterdam) **23D**, 3 (1986).
[14] P. Grassberger and Y. C. Zhang, Physica (Amsterdam) **224A**, 169 (1996); C. A. Voigt and R. M. Ziff, Phys. Rev. E **56**, R6241 (1997); for a useful list of the exponents, see M. A. Muñoz, R. Dickman, A. Vespignani, and S. Zapperi, Phys. Rev. E **59**, 6175 (1999).
[15] Kai *et al.* reported hysteresis of the DSM1-DSM2 transition showing algebraic dependence on the ramp rate of V [12]. This may seem in contradiction with the DP framework, but this scaling of hysteresis loops turns out to be one aspect of DP criticality under the presence of a tiny residual probability for spontaneous nucleation of DSM2 patches. This is detailed in K. A. Takeuchi, arXiv:0706.4152.